Volume 50 | Number 67 | 28 August 2014 | Pages 9419–9612

ChemComm

Chemical Communications

www.rsc.org/chemcomm

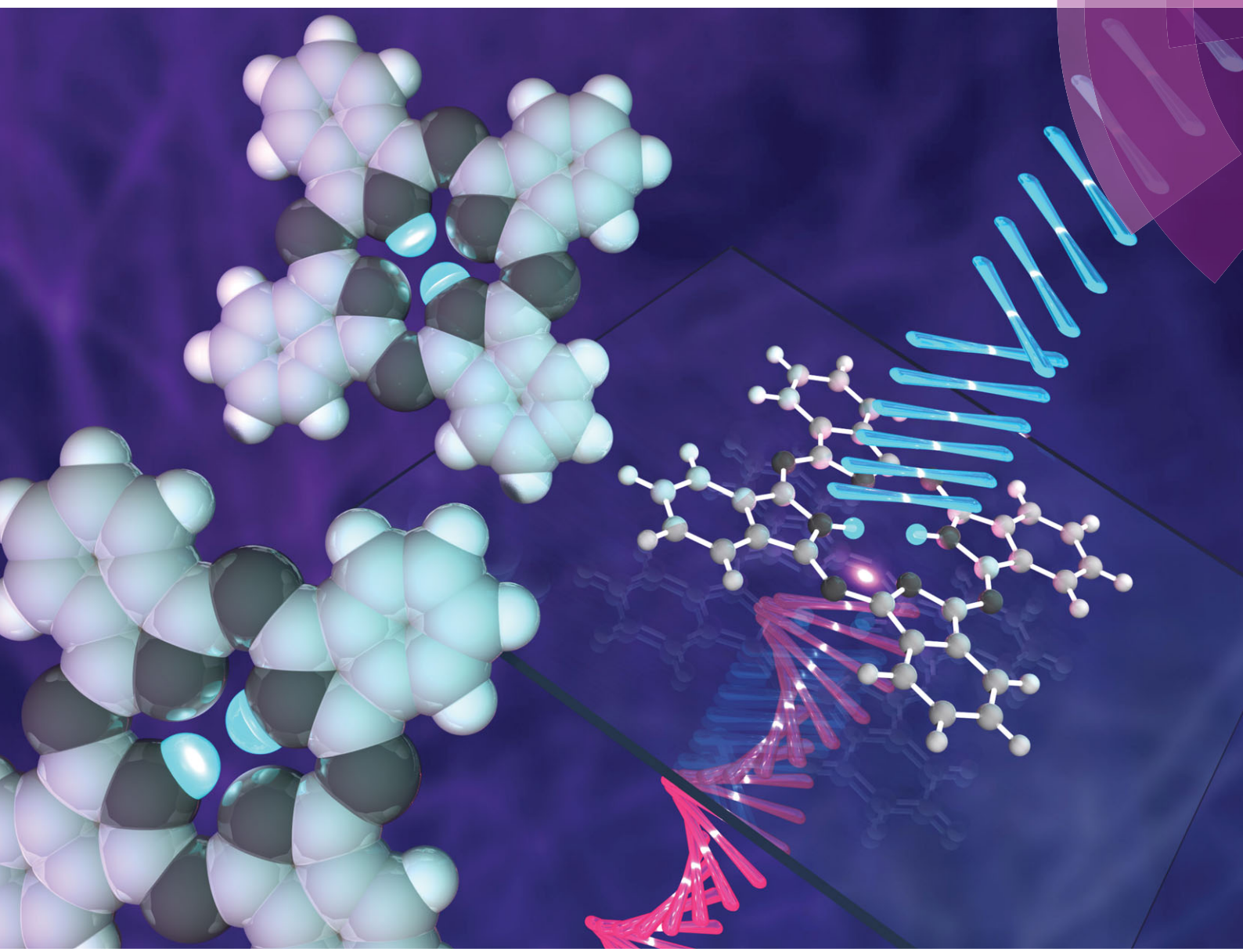

ISSN 1359-7345

ROYAL SOCIETY OF CHEMISTRY

COMMUNICATION

Hiroyuki Noji *et al.*

Real-time fluorescence visualization of slow tautomerization of single free-base phthalocyanines under ambient conditions

ChemComm

COMMUNICATION

View Article Online
View Journal | View Issue

Cite this: *Chem. Commun.*, 2014, 50, 9443

Received 8th April 2014,
Accepted 20th May 2014

DOI: 10.1039/c4cc02574a

www.rsc.org/chemcomm

Real-time fluorescence visualization of slow tautomerization of single free-base phthalocyanines under ambient conditions†‡

T. Ikeda,[ab] R. Iino[ab] and H. Noji*[ab]

The emission transition dipole moments of single-molecule free-base phthalocyanines at an air/glass interface were visualized using defocused wide-field fluorescence microscopy at a temporal resolution of 100–200 ms. Isolated molecules showed slow proton tautomerization, which is consistent with previous theoretical calculations in the gas phase, which predicted large activation energies.

Phthalocyanines (Pcs) are macrocyclic molecules with π-electron conjugation similar to that of hemes in biological systems. Owing to their characteristic light absorption/emission, electronic properties, and planar structures, Pc derivatives often play a key role in various chemical systems such as electronic devices, catalysts, supramolecules, and in scanning tunnelling microscopy imaging.[1–7] Additionally, tautomerization through inner-proton transfer in the central cavity of the molecule is known in the free-base phthalocyanine (**H_2Pc**) both theoretically[8–12] and experimentally[13–16] (Fig. 1A). Interestingly, the orientation of the emission transition dipole moment (ETDM, or molecular orbital) rotates 90° with this tautomerization;[11–15] therefore, the applications of these molecules as a molecular memory and a conductivity switch were expected.[13–15] The timescale of the tautomerization of **H_2Pc** in the crystal state was estimated by NMR to be fast, that is, 0.01 ms at around room temperature.[16] On the other hand, by using density functional theory (DFT) calculations for the tautomerization of **H_2Pc** in the gas phase, a large activation energy of 64.2 kJ mol^{-1} (27 in k_BT_{289} units) has been predicted.[10] This suggests a much slower rate of tautomerization for isolated **H_2Pc** molecules. However, an early attempt to use fluorescence microscopy to visualize the ETDMs of single **H_2Pc**s embedded into polymers or attached to silica failed,[17] presumably because of the low rate of image acquisition (~100 s) compared with the rate of tautomerization. In this study, we report the real-time visualization of the ETDMs of single **H_2Pc**s using defocused wide-field microscopy at a temporal resolution of 100 ms.[18–23] We found that a **H_2Pc** derivative shows slow tautomerization at an air/octadecyl-group-modified glass interface, which is consistent with previous DFT calculations.

H_2Pc is a bright fluorescent dye that shows strong absorption around the red region (650–700 nm) and deep-red emission peaks (around 700 nm)[24] (Fig. 1B). We first tried visualizing the fluorescence emission from single **H_2Pc** molecules at the air/bare-glass interface. **H_2Pc** was bound to bare glass by the contact of toluene solution with an optically clean glass surface (see ESI‡). A wide-field fluorescence microscope equipped with a circularly polarized, 638 nm red laser light for excitation was used for observation. A deep red fluorescence emission signal (>650 nm) was imaged using an EMCCD camera at a time resolution of 100 or 200 ms (see ESI‡).

Fig. 2A–D show fluorescence images obtained with various concentrations of **H_2Pc** in toluene at the binding step. The density of spots decreased with decreasing **H_2Pc** concentration (Fig. 2A–D). In the absence of **H_2Pc** (Fig. 1D), no clear spots were observed, indicating that these spots were not signals from contaminants in the solvent. The intensity profile of each spot was fitted well with a Gaussian curve (Fig. 2C, two insets). The full-width at half-maximum (FWHM) was 578 ± 64 nm (mean ± SD for $N = 10$ spots). Typical time courses of the fluorescence intensity of single spots are plotted in Fig. 2E. Single-step photo-bleaching, in which spots lost their intensity suddenly, were observed in the time courses. Such single-step photo-bleaching is a typical property of single fluorophores in single-molecule imaging. The signal-to-noise ratio (SNR)[25,26] in the time courses was 7.1 ± 3.5 at 5 frames per second (fps) (mean ± SD for $N = 18$ spots). To further confirm that the observed spots corresponded to the fluorescence emission from single-molecule **H_2Pc**, the distribution of the durations before the photo-bleaching was investigated by counting the number of spots in a unit area *versus* time. The distribution was reproduced well by a single-exponential decay, indicating a stochastic first-order reaction consistent with irreversible photo-bleaching of single molecules (Fig. 2F). Under our experimental conditions

[a] *Department of Applied Chemistry, School of Engineering, The University of Tokyo, Tokyo, Japan. E-mail: hnoji@appchem.t.u-tokyo.ac.jp*
[b] *Core Research for Evolutional Science and Technology, Japan Science and Technology Agency, Tokyo, Japan*

† Dedicated to Professor Seiji Shinkai on the occasion of his 70th birthday.

‡ Electronic supplementary information (ESI) available: Details of optics and sample preparation. See DOI: 10.1039/c4cc02574a

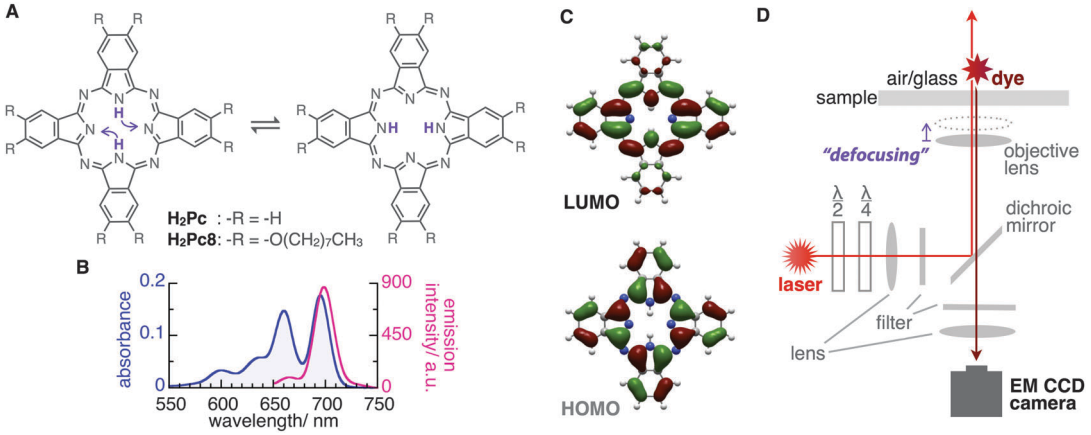

Fig. 1 (A) Schematic illustration of tautomerization of phthalocyanines by inner-proton transfer. (B) Absorption (optical path length: 10 mm) and emission spectra (excitation wavelength: 638 nm) of **H_2Pc** in *o*-dichlorobenzene (1.1 μM) at 298 K. Strong peaks at 660, 695 nm for absorption and 699 nm for emission. (C) The HOMO and LUMO of **H_2Pc** generated by DFT calculations at the RB3LYP/6-31G(d,p) level. (D) Schematic illustration of optics for visualization of fluorescence emission from single phthalocyanines.

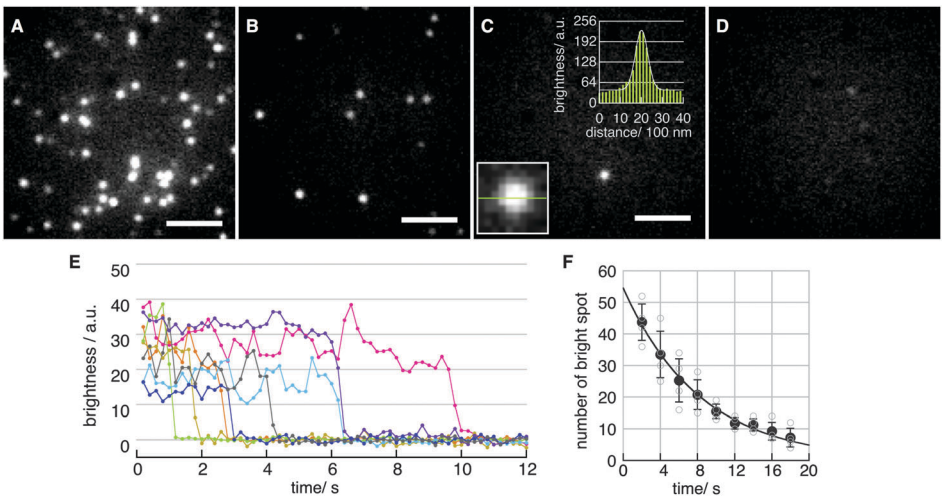

Fig. 2 (A–D) Fluorescence images of **H_2Pc** at the air/bare-glass interface. Scale bar: 5 μm. Laser power: 11.6 μW μm^{-2}. Acquisition time for each image: 200 ms. Initial concentration of **H_2Pc** in toluene at the binding step was (A) 1000 nM, (B) 100 nM, (C) 10 nM, and (D) zero. The two insets in (C) show the intensity profile on the cross section of the bright spot in the same image. (E) Typical time courses of fluorescence intensity of spots. The intensity for a single spot was determined as a mean value of pixel intensity in a unit area (10 × 10 pixels). The signal-to-noise ratio (SNR) of each time course was 7.1 ± 3.5 for 18 spots. (F) Distribution of duration times of photo-bleaching. Change in the number of spots (empty circles) in a unit area (128 × 128 pixel, 424 μm^2) was measured. Mean value (filled circles) was fitted by single-exponential decay ($A \exp(-k_{bleach} \cdot t)$), where k_{bleach} = 0.12 s^{-1}, A = 54.6, and R^2 = 0.993. Time constant τ ($1/k_{bleach}$) was 8.2 s.

(room temperature, laser power of 11.6 μW μm^{-2}), the time constant for photo-bleaching was 8.2 s. From these results, we concluded that fluorescence emission from single **H_2Pc** molecules was visualized successfully with a temporal resolution of 100 ms.

Next, we determined directly the ETDM of single **H_2Pc** molecules through defocused wide-field imaging.[18–23] The height of the objective lens was moved by ~1 μm toward the sample plane to generate defocused images[18] (Fig. 1D). A typical transition process from the focused image to the defocused image of single **H_2Pc** molecules bound to a C18-glass, surface-modified with octadecyl groups (see ESI‡), is shown in Fig. 3A. As shown in Fig. 3B, anisotropic double-lobe-like patterns of single **H_2Pc** molecules were observed in the defocused image. The double-lobe images are similar to those observed in the defocused imaging of fluorescent dyes such as rhodamine[19] and perylenediimide,[20–23] attached to a glass surface. In these dyes, it is known that the orientation of the double-lobe image indicates that of the ETDM.[18–23] In theoretical calculations of the molecular orbitals of **H_2Pc**, the LUMO (lowest unoccupied molecular orbital) has anisotropy in connection with the position of the two hydrogen atoms in the molecule (Fig. 1C).[11,12] Although the two isomers are chemically identical,[8–10] the tautomers are distinguishable because the anisotropy rotates by 90°. Therefore, the observation of a double-lobe pattern strongly suggests that both tautomerization and rotational motion of **H_2Pc** on C18-glass are much slower than the timescale of observation (100 ms). On the other hand, not the double-lobe but a donut pattern was

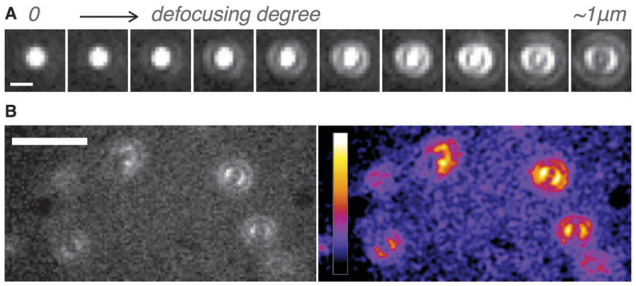

Fig. 3 (A) Transition process from the focused image to the defocused image of **H_2Pc** on C18-glass. Laser power: 9.0 μW μm^{-2}. Scale bar: 1 μm. Acquisition time for each image: 1.0 s. (B) Defocused images of **H_2Pc** at air/C18-glass interfaces. The image on the right is contrasted and pseudo-colored (left images). Scale bar: 5 μm. Laser power: 4.5 μW μm^{-2}. Acquisition time for each image: 100 ms.

observed when the bare glass was used (not shown). Silanol groups of the silicate glass and adsorbed water on the surface may increase the rate of tautomerization of **H_2Pc**. Alternatively, **H_2Pc** may show much faster molecular rotation on the bare glass.

Although the double-lobe-like patterns of **H_2Pc** were observed, **H_2Pc** itself was not suitable for kinetic analysis owing to the slow lateral diffusion on the surface of the C18-glass on longer timescales (for 10 s, see Movie S1, ESI‡). Therefore, we used a **H_2Pc** derivative, **H_2Pc8**, which has eight octyl groups at peripheral positions of **H_2Pc** (Fig. 1A), expecting a stronger van der Waals interaction with C18-glass. The optical properties such as absorption and emission of **H_2Pc8** were similar to those of **H_2Pc** (see ESI‡), and, as expected, the lateral diffusion of **H_2Pc8** on C18-glass was suppressed effectively (see Movie S1, ESI‡). In defocused imaging of **H_2Pc8** at the air/C18-glass interface, most molecules showed the double-lobe pattern (92% of 789 spots; the residual 8% showed the donut pattern). Basically, the orientation of the double-lobe patterns was stationary and not changed during observation, indicating that the time-scale of tautomerization and molecular rotation of **H_2Pc8** on the C18-glass is much longer than that of photo-bleaching (8.2 s). On the other hand, of the defocused images that formed the double-lobe pattern, 13% (97 spots) showed switching to another orientation during observation (Fig. 4A, Movie S2, ESI‡). The origin of two different populations, stationary and switchable, is unknown so far. They may come from the inhomogeneous properties of the C18 glass surface to which **H_2Pc8**s are bound. A montaged image and a time course of the ETDM angle are shown in Fig. 4B–D. In the histogram of angle distribution, two peaks appeared in most cases (Fig. 4E). The difference in the angle between the two peaks was defined as the step angle, $\Delta\theta$, for each molecule. The distribution of $\Delta\theta$ is shown in Fig. 4F. Through fitting with a Gaussian curve, the step angle for **H_2Pc8** was determined to be 89 ± 16° (mean ± SD, N = 81 molecules), strongly suggesting that switching arises from tautomerization (Fig. 1A and C). The average time before switching to the next orientation was 2.3 ± 3.9 s (mean ± SD, N = 265 events). Our results indicate that the rate of tautomerization is very slow compared with the reported value for **H_2Pc** in the crystal state (≈0.01 ms at 298 K).[16] In other words, the timescale of the tautomerization of **H_2Pc8** at the air/C18-glass interface at room temperature is a few seconds or longer. The activation energies of the fast tautomerization of **H_2Pc** in the crystal state have been estimated to be 39 and 32 kJ mol^{-1} (16 and 13 in k_BT_{289} units) for the α- and β-form crystals, respectively.[16] However, through DFT calculations for the tautomerization of **H_2Pc** in the gas phase, a larger value of 64.2 kJ mol^{-1} (27 in k_BT_{289} units) has been predicted.[10] The electronic state in the crystal must be different from that in a fully isolated environment such as the gas phase because of intermolecular π–π interactions caused by molecular

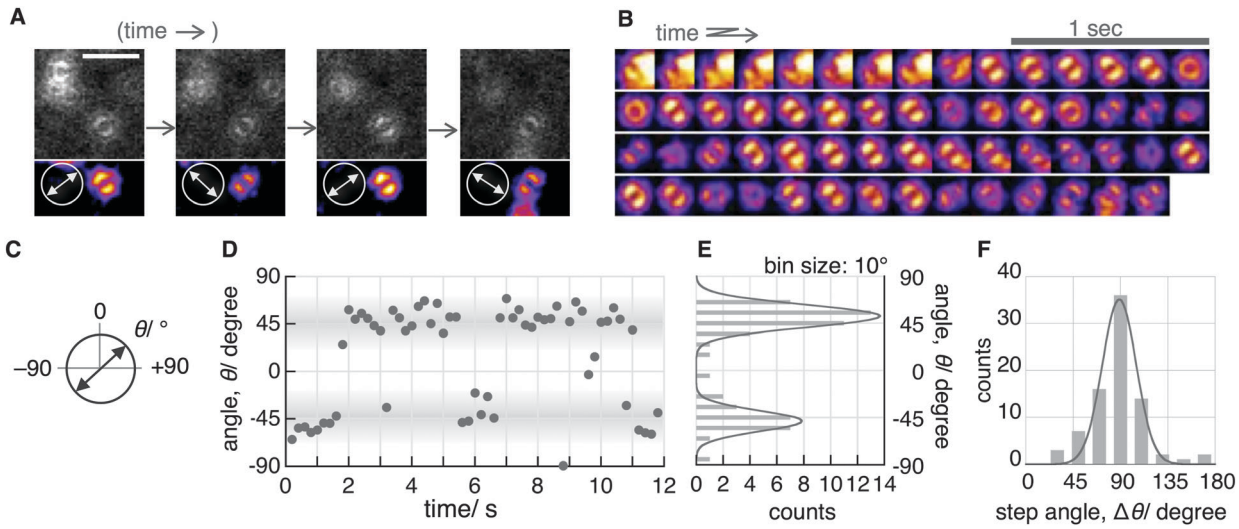

Fig. 4 Slow switching of the ETDM of **H_2Pc8** at the air/C18-glass interface. (A) Sequential images of the same molecule showing switching. Scale bar: 4 μm. Laser power: 11.6 μW μm^{-2}. Acquisition time for each image: 200 ms. Bottom images are contrasted and pseudo-colored. Orientation of arrows in circles indicates the ETDM direction. (B) A montaged image of recorded movie at 5 fps. (C) Definition of orientation. (D) Angle time course and (E) angle distribution of single molecules shown in B. (F) Histogram of step angle, $\Delta\theta$. $\Delta\theta$ was estimated to be 89 ± 16° (mean ± SD, N = 81 molecules) by fitting with a Gaussian.

packing.[27,28] It is highly likely that our experimental conditions using the air/glass interface for the visualization of isolated **H_2Pc**s are close to the gas-phase conditions used in the DFT calculations. If the frequency factor (A) in the Arrhenius equation ($k = A\exp(-E_a/k_BT)$; k, rate constant; E_a, activation energy in k_BT unit; k_B, Boltzmann constant; T, temperature in K) is similar to the experimental value (10^{11}–10^{12} s^{-1})[16] in the crystal phase; the value by DFT means that k is much smaller. It corresponds to a time constant of 0.4–4.0 s. Therefore, our experimental results are consistent with those of DFT calculations.

We visualized the fluorescence emission from single free-base phthalocyanines at the air/glass interface under ambient conditions using optical microscopy. The single **H_2Pc** was imaged as bright spots for several seconds with a temporal resolution of 100 ms. Tautomerization of **H_2Pc8** on a timescale much longer than 100 ms was observed at the air/C18-glass interface. Furthermore, intermittent ETDM switching with a step size of 90° was captured. We concluded that the timescale of tautomerization by proton transfer in **H_2Pc8** at the air/C18-glass interface at room temperature is a few seconds or longer. **H_2Pc** would contribute to develop a molecular memory or a switch which works under ambient conditions if we can control this slow tautomerization by further chemical modifications and/or external stimuli.

This work was supported by CREST (Core Research for Evolutional Science and Technology) of the Japan Science and Technology Agency, and Grants-in-Aid for Scientific Research (No. 18074005 to H. N. and No. 24651167 to R. I.) from the Ministry of Education, Science, Sports, and Culture of Japan.

Notes and references

1 G. de la Torre, C. G. Claessens and T. Torres, *Chem. Commun.*, 2007, 2000–2015.
2 K. J. Baeg, M. Binda, D. Natali, M. Caironi and Y. Y. Noh, *Adv. Mater.*, 2013, **25**, 4267–4295.
3 A. B. Sorokin, *Chem. Rev.*, 2013, **113**, 8152–8191.
4 G. Bottari, O. Trukhina, M. Ince and T. Torres, *Coord. Chem. Rev.*, 2012, **256**, 2453–2477.
5 P. D. Frischmann, K. Mahata and F. Wurthner, *Chem. Soc. Rev.*, 2013, **42**, 1847–1870.
6 T. Komeda, H. Isshiki and J. Liu, *Sci. Technol. Adv. Mater.*, 2010, **11**, 054602.
7 G. Baffou, A. J. Mayne, G. Comtet, G. Dujardin, L. Stauffer and P. Sonnet, *J. Am. Chem. Soc.*, 2009, **131**, 3210–3215.
8 K. A. Nguyen and R. Pachter, *J. Phys. Chem. A*, 2000, **104**, 4549–4552.
9 H. Cortina, M. L. Senent and Y. G. Smeyers, *J. Phys. Chem. A*, 2003, **107**, 8968–8974.
10 T. Strenalyuk, S. Samdal and H. V. Volden, *J. Phys. Chem. A*, 2008, **112**, 4853–4860.
11 A. V. Kukhta, E. E. Kolesnik, I. N. Kukhta, A. E. Pochtenny, V. K. Dolgiy, G. A. Mousdis and N. Psaroudakis, *Synth. Met.*, 2010, **160**, 2361–2365.
12 A. Lee, D. Kim, S. H. Choi, J. W. Park, J. Y. Jaung and D. H. Jung, *Mol. Simul.*, 2010, **36**, 192–198.
13 A. Sperl, J. Kroger and R. Berndt, *Angew. Chem., Int. Ed.*, 2011, **50**, 5294–5297.
14 P. Liljeroth, J. Repp and G. Meyer, *Science*, 2007, **317**, 1203–1206.
15 T. C. Niu and A. Li, *J. Phys. Chem. Lett.*, 2013, **4**, 4095–4102.
16 B. Wehrle and H. H. Limbach, *Chem. Phys.*, 1989, **136**, 223–247.
17 A. M. Chizhik, R. Jager, A. I. Chizhik, S. Bar, H. G. Mack, M. Sackrow, C. Stanciu, A. Lyubimtsev, M. Hanack and A. J. Meixner, *Phys. Chem. Chem. Phys.*, 2011, **13**, 1722–1733.
18 M. Bohmer and J. Enderlein, *J. Opt. Soc. Am. B*, 2003, **20**, 554–559.
19 D. Nishimura, Y. Takashima, H. Aoki, T. Takahashi, H. Yamaguchi, S. Ito and A. Harada, *Angew. Chem., Int. Ed.*, 2008, **47**, 6077–6079.
20 J. A. Hutchison, H. Uji-i, A. Deres, T. Vosch, S. Rocha, S. Muller, A. A. Bastian, J. Enderlein, H. Nourouzi, C. Li, A. Herrmann, K. Mullen, F. De Schryver and J. Hofkens, *Nat. Nanotechnol.*, 2014, **9**, 131–136.
21 H. Uji-i, S. M. Melnikov, A. Deres, G. Bergamini, F. De Schryver, A. Herrmann, K. Mullen, J. Enderlein and J. Hofkens, *Polymer*, 2006, **47**, 2511–2518.
22 P. Dedecker, B. Muls, A. Deres, H. Uji-i, J. Hotta, M. Sliwa, J. P. Soumillion, K. Mullen, J. Enderlein and J. Hofkens, *Adv. Mater.*, 2009, **21**, 1079–1090.
23 A. Deres, G. A. Floudas, K. Mullen, M. Van der Auweraer, F. De Schryver, J. Enderlein, H. Uji-i and J. Hofkens, *Macromolecules*, 2011, **44**, 9703–9709.
24 P. G. Seybold and M. Gouterma, *J. Mol. Spectrosc.*, 1969, **31**, 1–13.
25 H. Ueno, S. Nishikawa, R. Iino, K. V. Tabata, S. Sakakihara, T. Yanagida and H. Noji, *Biophys. J.*, 2010, **98**, 2014–2023.
26 The definition is as follows: $SNR = (I_S + I_{BG})/(\sigma_S^2 - \sigma_{BG}^2)^{1/2}$; I_S, signal intensity; I_{BG}, background intensity; σ_S^2, variance for signal; σ_{BG}^2, variance for background.
27 J. Janczak and R. Kubiak, *J. Alloys Compd.*, 1992, **190**, 121–124.
28 R. Kubiak and J. Janczak, *J. Alloys Compd.*, 1992, **190**, 117–120.

